

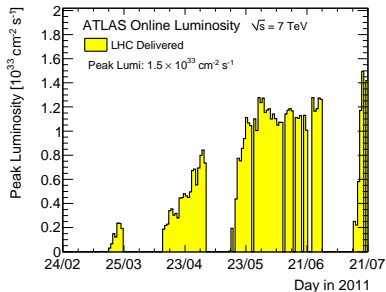
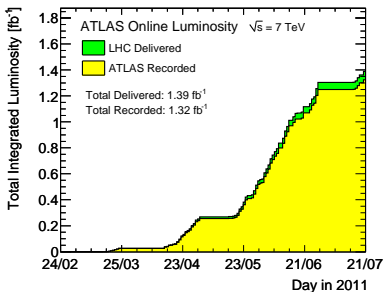
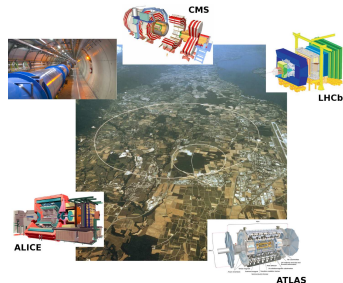
ATLAS status $b\bar{b}-\gamma\gamma$

J-F. Marchand
on behalf of the ATLAS collaboration

Higgs Hunting 2011 - 28/07/2011

- **Data taking in 2011**

- **Integrated luminosity : 1.39 fb^{-1}** delivered
- Peak luminosity : $1.5 \cdot 10^{33} / \text{cm}^2 / \text{s}^2$
- Max. luminosity in one fill : 62 pb^{-1}
(Total 2010 : 48.1 pb^{-1})
- Integrated luminosity of $3\text{-}4 \text{ fb}^{-1}$ by end of year ???



The ATLAS detector

Inner detector :

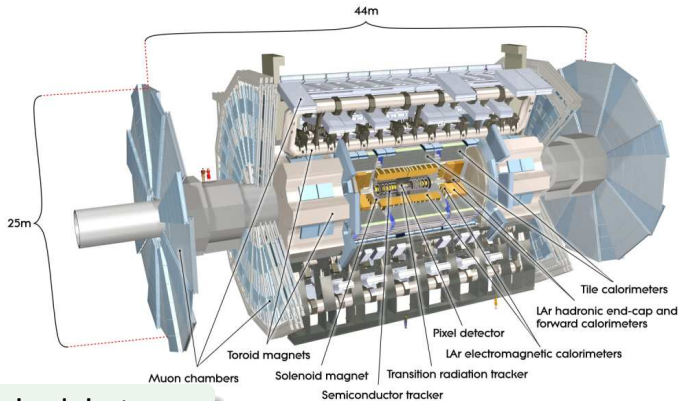
Pixel detector + SCT + TRT

$$\frac{\sigma_{pT}}{pT} \approx 0.05\% pT \oplus 1\%, |\eta| < 2.5$$

EM calorimeter :

Lead-LAr sampling calo. with accordion geometry

$$\frac{\sigma_E}{E} \approx \frac{10\%}{\sqrt{E}} \oplus 0.7\%, |\eta| < 3.2$$



Hadronic calorimeter :

Steel and scintillating tiles in the barrel, copper and liquid argon in end-caps

$$\frac{\sigma_E}{E} = \frac{50\%}{\sqrt{E}} \oplus 3\%, |\eta| < 3.2$$

$$\frac{\sigma_E}{E} = \frac{100\%}{\sqrt{E}} \oplus 10\%, 3.1 < |\eta| < 4.9$$

Muon spectrometer :

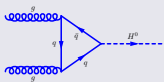
superconducting air-core toroid magnets, gas based muon chambers

$$\frac{\sigma_{pT}}{pT} \approx 2\% \text{ at } 50\text{GeV to } 10\% \text{ at } 1\text{TeV}, |\eta| < 2.7$$

Higgs hunting in ATLAS

Higgs boson production

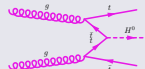
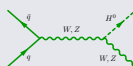
- gg fusion



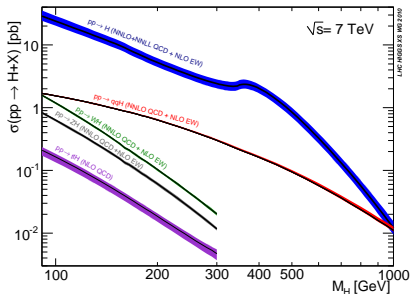
- Vector Boson Fusion (VBF)



- Associated production with W, Z or $t\bar{t}$



Cross-sections



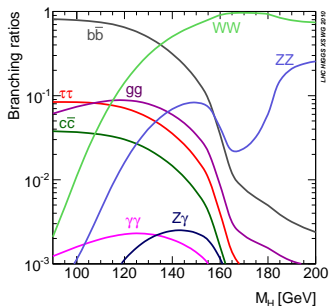
From "Handbook of LHC Higgs Cross Sections : 1. Inclusive Observables" arXiv :1101.0593

Higgs hunting in ATLAS

- This talk concentrates on SM Higgs searches in the low mass region ($110 < m_H < 150\text{GeV}$)
- Two different analyses are described :
 - $H \rightarrow b\bar{b}$

Dominant channel in the low mass region
Due to the large inclusive QCD backgrounds, detection of this decay is however extremely challenging
 - $H \rightarrow \gamma\gamma$

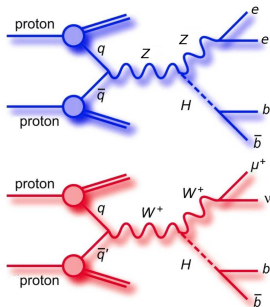
Small branching ratio
But simple signature and very good mass resolution



$H \rightarrow b\bar{b}$ analysis

- $H \rightarrow b\bar{b}$ searches in ZH/WH production
 - $ZH \rightarrow \ell\ell b\bar{b}$
 - $WH \rightarrow \ell\nu b\bar{b}$
- $\sigma_{WH} \approx 2 \times \sigma_{ZH}$
- But ZH less affected by top background

m_H (GeV)	$\sigma(WH)$ (pb)	$\sigma(ZH)$ (pb)	Branching Ratios $H \rightarrow b\bar{b}$
110	0.875	0.472	0.745
115	0.755	0.360	0.705
120	0.656	0.316	0.649
125	0.573	0.278	0.578
130	0.501	0.245	0.494



• Signature

- High p_T isolated leptons (+ E_T^{miss} for WH analysis)
- 2 b -jets

• Backgrounds

- W/Z +jets
- QCD multijets production
- Top quark production
- Dibosons WW, ZZ, ZW

Search for $H \rightarrow bb$ - Event selection

	$ZH \rightarrow \ell\ell b\bar{b}$		$WH \rightarrow \ell\nu b\bar{b}$	
	e channel	μ channel	e channel	μ channel
Kinematic cuts	$E_T^e > 20\text{GeV}$ $ \eta_{\text{cluster}}^e < 2.47$	$E_T^\mu > 20\text{GeV}$ $ \eta^\mu < 2.5$	$E_T^e > 25\text{GeV}$ $ \eta_{\text{cluster}}^e < 2.47$	$E_T^\mu > 25\text{GeV}$ $ \eta^\mu < 2.5$
Identification	medium	-	tight	-
Track impact parameters		$ d_0 < 1\text{mm}$ $ z_0 < 10\text{mm}$	$ d_0 < 0.1\text{mm}$ $ z_0 < 10\text{mm}$	
Track isolation	$\Sigma p_T^{\text{track}} (\Delta R < 0.2) < 0.1 p_T^\ell$			

To avoid double counting : e candidates within $\Delta R < 0.2$ of a selected μ are rejected

	$ZH \rightarrow \ell\ell b\bar{b}$	$WH \rightarrow \ell\nu b\bar{b}$
Trigger	Single lepton, di-lepton	Single lepton
Primary vertex	with ≥ 3 tracks	
Number of leptons	exactly two	exactly one
Mass cut	$76 < m_{\ell\ell} < 106\text{GeV}$	$m_T > 40\text{GeV}$
E_T^{miss} cut	$E_T^{\text{miss}} < 50\text{GeV}$	$E_T^{\text{miss}} > 25\text{GeV}$
Number of jets	≥ 2 , 2 leading jets b-tagged	exactly 2, b-tagged

$$m_T = \sqrt{2p_T^\ell p_T^\nu (1 - \cos(\phi^\ell - \phi^\nu))}$$

Single lepton trigger $p_T > 18\text{GeV}$ for μ , $p_T > 20\text{GeV}$ for e

Di-lepton trigger $p_T > 12\text{GeV}$

1.04fb⁻¹ used, after beam, detector and data-quality requirements

Background estimation

● $W + \text{jets}$

- Use m_{jj} from data as template
- Normalization from control region
 $40 < m_{b\bar{b}} < 80\text{GeV}$ and $140 < m < 250\text{GeV}$

● $Z + \text{jets}$

- Shape from MC
- Normalization from control region
 $40 < m_{b\bar{b}} < 80\text{GeV}$ and $140 < m < 250\text{GeV}$
- Control region : events with only one b -tagged jet

● Top production

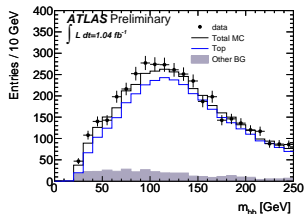
- Shape from MC
- Normalization for WH analysis : from $m_{b\bar{b}}$ sidebands ($40 < m_{b\bar{b}} < 80\text{GeV}$ and $140 < m < 250\text{GeV}$), x-checked $m_{b\bar{b}}$ in 3-jets bin
- Normalization for ZH analysis : from MC, checked in $m_{\ell\ell}$ control regions : $60 < m_{\ell\ell} < 76\text{GeV}$ or $106 < m_{\ell\ell} < 150\text{GeV}$

● QCD multijet events

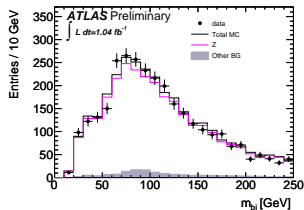
- Shape from a multijet enriched data sample
- Normalization from multicomponent fit to E_T^{miss} for WH , $m_{\ell\ell}$ for ZH

● Diboson : from MC

Top control region for WH analysis



Control region for ZH



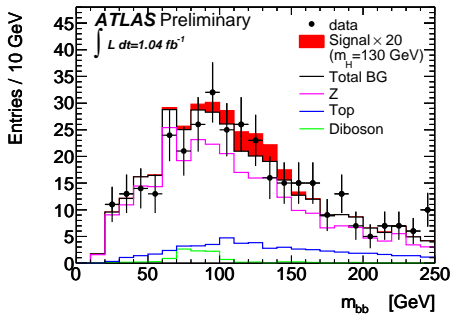
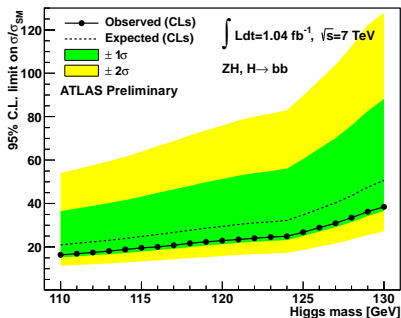
Systematic uncertainties

Source of Uncertainty	Effect on $ZH \rightarrow \ell\ell b\bar{b}$ signal		Effect on $WH \rightarrow \ell\nu b\bar{b}$ signal	
	$m_H = 115$ GeV	$m_H = 130$ GeV	$m_H = 115$ GeV	$m_H = 130$ GeV
Electron Energy Scale	< 1%	< 1%	1%	1%
Electron Energy Resolution	< 1%	< 1%	1%	1%
Muon Momentum Resolution	1%	3%	4%	1%
Jet Energy	9%	7%	1%	3%
Jet Energy Resolution	< 1%	< 1%	1%	1%
Missing Transverse Energy	2%	2%	2%	3%
<i>b</i> -tagging Efficiency	16%	17%	16%	17%
<i>b</i> -tagging Mis-tag Fraction	< 1%	< 1%	3%	3%
Electron Efficiency	1%	1%	1%	1%
Muon Efficiency	1%	1%	1%	1%
Luminosity	4%	4%	4%	4%
Higgs Cross-section	5%	5%	5%	5%

- Dominant systematic error from *b*-tagging efficiency in both analyses
- Followed by jet energy

Here *Jet Energy* refers to jet energy scale, pile-up and *b*-jet energy scale uncertainties; *Electron Efficiency* to trigger, reconstruction and selection efficiencies and *Muon Efficiency* refers to the muon trigger and selection efficiencies.

Results - $ZH \rightarrow llbb$

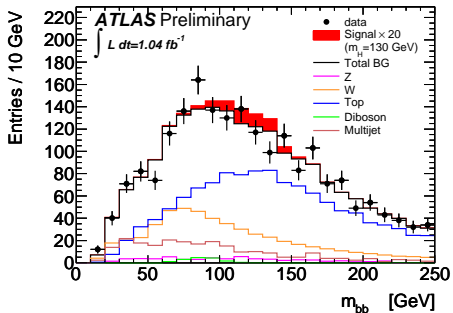
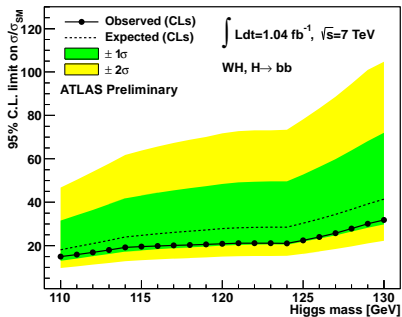


- The modified frequentist approach CL_s ¹ is used

- Good description of the background
- No excess observed
- Single-channel observed exclusion of 15-35 times the SM

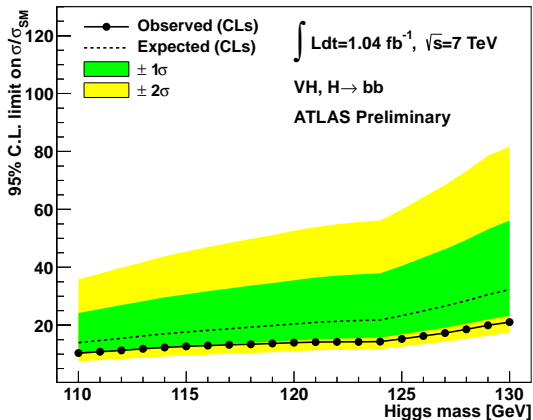
¹ Presentation of search results : the CLs technique A. L. Read 2002 J. Phys. G : Nucl. Part. Phys. 28 2693

Results - $WH \rightarrow \ell\nu bb$



- Good description of the background
- No excess observed
- Single-channel observed exclusion of 15-30 times the SM

Results - WH and ZH combined

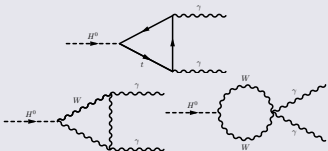


- No excess observed
- Observed exclusion limits 10-20 times the SM between 110 and 130GeV

$H \rightarrow \gamma\gamma$ analysis

- $H \rightarrow \gamma\gamma$ is one of the most promising discovery channels for a SM Higgs boson in low mass region ($114 < m_H < 150\text{GeV}$)

Signal



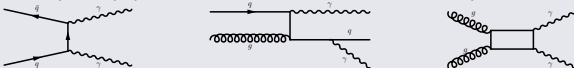
- Small branching ratio ($2.25 \cdot 10^{-3}$ for $m_H = 120\text{GeV}$)

BUT

- Simple signature
 - Very good mass resolution ($\approx 1.5\text{GeV}$)
- Need good photon reconstruction/identification
→ Need proper conversion handling
→ Need good photon direction measurement

Background

- Irreducible : $\gamma\gamma(+\text{jets})$ (Born, fragmentation processes, box)



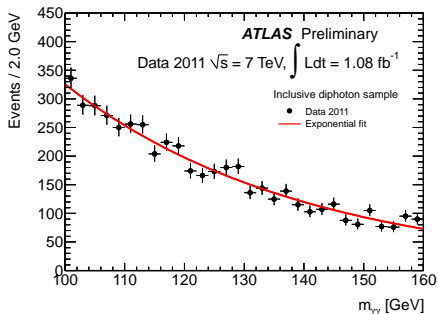
- Reducible : $\gamma/\text{jet}(s)$, $\text{jet}(s)/\text{jet}(s)$
- Drell-Yan events : both e misidentified as γ

Event selection

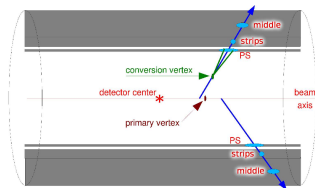
- 1.08fb^{-1} used, after beam, detector and data-quality requirements
- Di-photon trigger : $E_T > 20\text{GeV}$ with loose identification cuts
- At least one primary vertex with ≥ 3 tracks
- **2 photon candidates** are selected
 - $E_T > 40\text{GeV}$ and $E_T > 25\text{GeV}$
 - $|\eta| < 2.37$ excluding transition region ($1.37 < |\eta| < 1.52$)
 - "Tight" identification cuts
 - Calorimetric isolation (cone $\Delta R < 0.4$) $< 5\text{GeV}$
 - Exclude γ in problematic region of the calorimeter

Compute **invariant mass** of photon pair

- Photon angle : from interaction vertex and γ impact point in the calorimeter
- Interaction vertex position determined only using γ candidates
 - Use of calo. pointing + conversion vtx
 - Robust against pile-up interactions

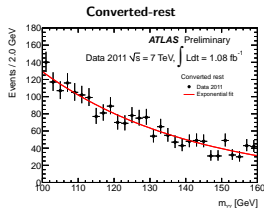
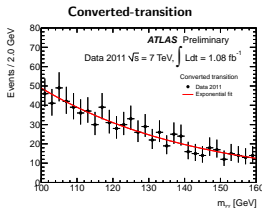
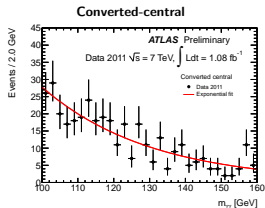
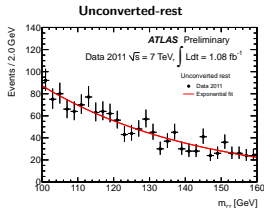
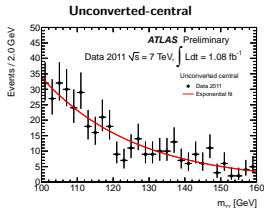


5063 events for 1.08fb^{-1} with
 $100 < m_{\gamma\gamma} < 160\text{GeV}$

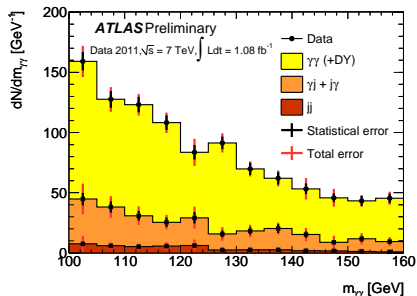


Event categorisation

- Inclusive sample divided into **5 categories with different $m_{\gamma\gamma}$ resolution and S/B**
→ signal rate sensitivity improved by $\approx 15\%$ for $m_H = 120\text{GeV}$
- Definition of the 5 categories
 - **Unconverted-central** : 2 unconv. γ in the central barrel calorimeter ($|\eta| < 0.75$)
 - **Unconverted-rest** : 2 unconv. γ , ≥ 1 γ is not central
 - **Converted-central** : ≥ 1 conv. γ , central
 - **Converted-transition** : ≥ 1 conv. γ and ≥ 1 γ near the transition between barrel and end-cap ($1.3 < |\eta| < 1.75$)
 - **Converted-rest** : all other events with ≥ 1 conv. γ



- **Double side-band method** applied to measure the fake photon background components directly from the data
 - exploits relaxed isolation and identification cuts, relying on the fact that the rejections from these 2 cuts are independent



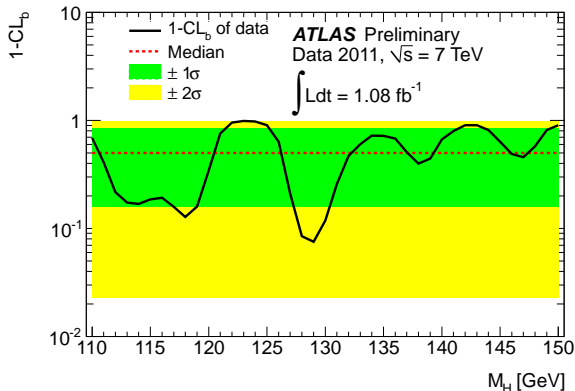
- **Other methods have been used to cross-check the purity estimate**
 - Using template fits of the γ isolation distribution, where both signal and background templates are derived from data
 - Results in agreement

Uncertainties on the signal yield	Total $\pm 12\%$
Reconstruction and identification efficiency	$\pm 11\%$
Isolation cut efficiency	$\pm 3\%$
Trigger efficiency	$\pm 1\%$
Luminosity	3.7%
Effect of p_T^H modelling on the kinematical cut acceptance	1%

Uncertainties on the invariant mass resolution	Total $\pm 14\%$
Constant term of the cluster energy resolution	$\pm 12\%$
Photon calibration from extrapolation of energy scale calibration of electrons	$\pm 6\%$
Contribution of pileup fluctuations to the cluster energy measurement	$< 3\%$
Photon angle measurements	1%

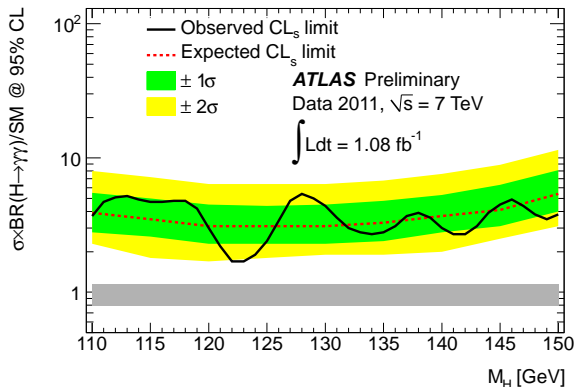
- *Uncertainties on the invariant mass resolution applied to both Crystal Ball (CB) and wide gaussian resolution parameters*
- These systematics uncertainties are taken as fully correlated between the different categories
- Impact of non-correlated systematic uncertainties studied and found to have negligible impact on the analysis

- Data compared to B and S+B hypothesis using a profile likelihood test statistic
- Background modelled by an exponentially falling invariant mass distribution determined by 2 nuisance parameters per category (normalisation and exp. negative slope) which are left free in the fit
- Signal modelled by a CB + wide gaussian, fixing the fraction of events in each category to the MC predictions
- Fitted parameters for the signal are :
 - overall signal strength relative to the SM prediction and
 - nuisance parameters on the predicted event yield
 - mass resolution which have gaussian constraints in the fit
- Fit performed every 1GeV in Higgs boson mass hypothesis
- Signal parameters are interpolated from the fully simulated samples



- No indication of significant excess
- The minimal value of $1 - \text{CL}_b$ value of the background upward fluctuation is $\approx 8\%$ for $m_{\gamma\gamma} \approx 129\text{GeV}$
- The probability for such an excess to appear anywhere in the investigated mass range is around 50%, for the background only hypothesis

Exclusion limits using CL_s method



- The modified frequentist approach CL_s ² is used
- The theoretical uncertainty on the predicted SM σ -section is not included in the experimental limit but shown as a band around 1

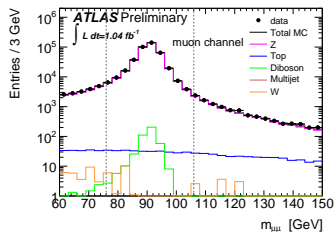
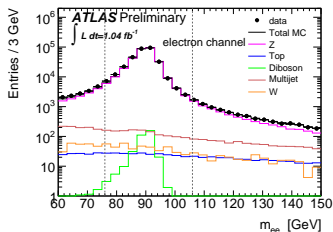
- Exclusion of 2 to 6 times the SM
- Fluctuations of observed limit consistent with expected statistical fluctuations

² Presentation of search results : the CL_s technique A. L. Read 2002 J. Phys. G : Nucl. Part. Phys. 28 2693

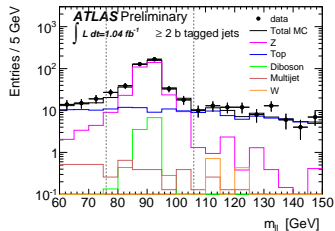
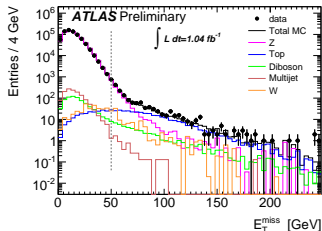
- Results using $> 1\text{fb}^{-1}$ of pp collision data at $\sqrt{s} = 7\text{TeV}$ in ATLAS
- $H \rightarrow b\bar{b}$ analysis and results have been presented
 - No excess observed
 - Exclusion limits 10 to 20 times the SM
- $H \rightarrow \gamma\gamma$ analysis and results have been presented
 - No indication of significant excess
 - Fluctuations are compatible with statistical fluctuations around the expected median limit in case of no signal
 - Exclusion of 2 to 6 times the SM

BACKUP

$H \rightarrow bb$ selection

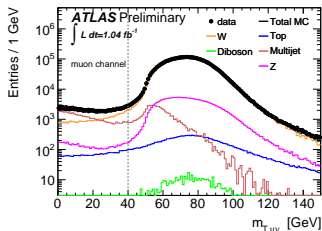
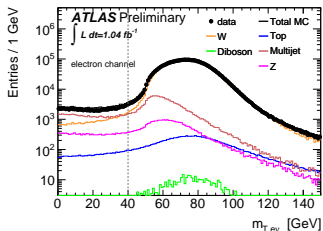
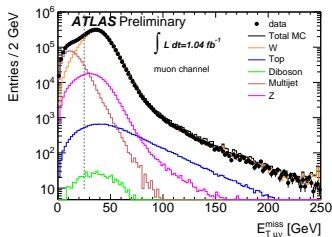
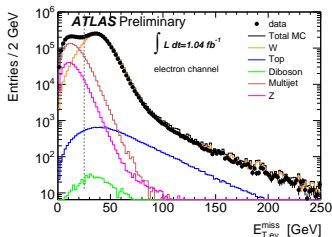


Distributions of the $m_{\ell\ell}$ for the ZH analysis for electrons (left) and muons (right)

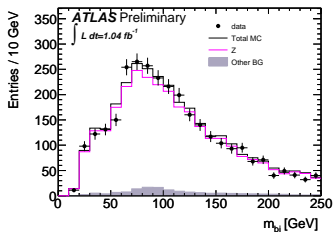


The distribution of E_T^{miss} (left) for the $ZH \rightarrow \ell\ell b\bar{b}$ search before the E_T^{miss} cut is applied. The di-lepton invariant mass ($m_{\ell\ell}$) distribution (right) after applying the low E_T^{miss} cut and requiring at least two high p_T b -tagged jets.

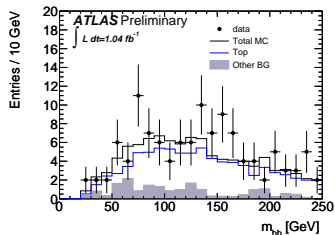
$H \rightarrow bb$ selection



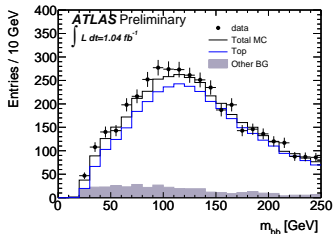
The distributions of E_T^{miss} (top) before the cut is applied in the $WH \rightarrow \ell\nu b\bar{b}$ analysis. The distribution of the transverse mass (bottom) shown after the cut on E_T^{miss} . The plots are shown for electrons (left column) and muons (right column), for the WH selection.



The invariant mass formed from the two highest p_T jets where one jet is b -tagged, for the ZH analysis.



The invariant mass formed from two b -tagged jets, using the sidebands of the $m_{\ell\ell}$ distribution, for the ZH analysis.



The di- b -jet invariant mass for the control region for top-quark events in the $WH \rightarrow \ell\nu b\bar{b}$ analysis where the requirement on the maximum number of jets is relaxed from two to three.

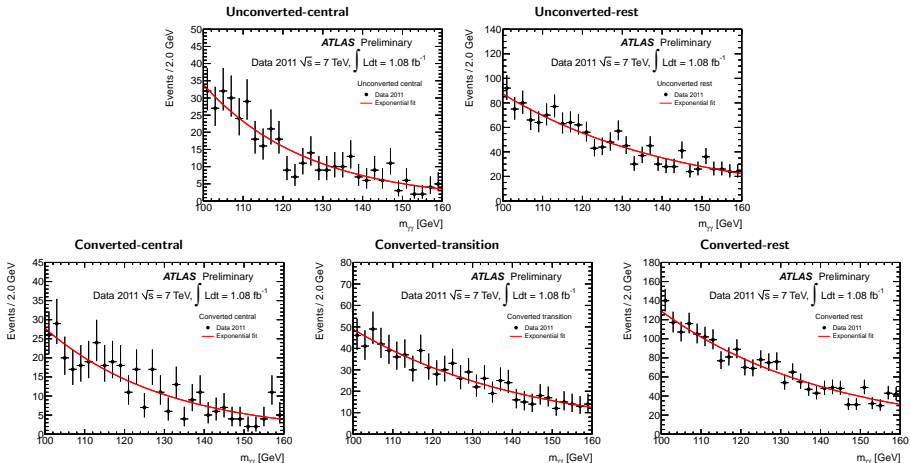
Sources of detector and reconstruction-related systematic uncertainties

Source of Uncertainty	Treatment in analysis
Jet Energy Scale (JES)	2 – 7% as a function of p_T and η
Jet Pile-up Uncertainty	2 – 7% as a function of p_T and η
b-quark Energy Scale	2.5%
Jet Energy Resolution	5 – 12%
Electron Selection Efficiency	0.7 – 3% as a function of p_T , 0.4 – 6% as a function of η
Electron Trigger Efficiency	0.4 – 1% as a function of η
Electron Reconstruction Efficiency	0.7 – 1.8% as a function of η
Electron Energy Scale	0.1 – 6% as a function of η , pileup, material effects etc.
Electron Energy Resolution	Sampling term 20%, a small constant term has a large variation with η
Muon Selection Efficiency	0.2 – 3% as a function of p_T
Muon Trigger Efficiency	< 1%
Muon Momentum Scale	2 – 16% η -dependent systematic on scale
Muon Momentum Resolution	p_T and η -dependent resolution smearing functions, systematic $\leq 1\%$
b-tagging Efficiency	5 – 14% as a function of p_T
b-tagging Mis-tag Fraction	8 – 12% as a function of p_T and η
Missing Transverse Energy	Add/subtract object uncertainties in E_T^{miss}

Sources of non-detector-related systematic uncertainties

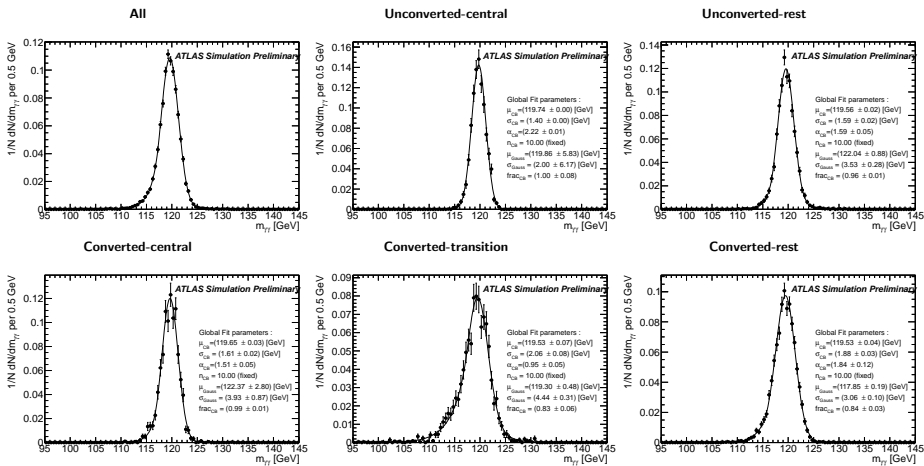
Source of Uncertainty	Treatment in analysis	
	ZH	WH
Luminosity	3.7%	3.7%
Higgs cross-section	5%	5%
Background norm. and shape :		
Top	9%	6%
Z+jets	11% plus shape	11%
W+jets	negligible	14% plus shapes
ZZ	11%	negligible
WZ	11%	11%
WW	negligible	11%
QCD multijets	100%	50%

$H \rightarrow \gamma\gamma$ - Invariant mass in data - 5 categories



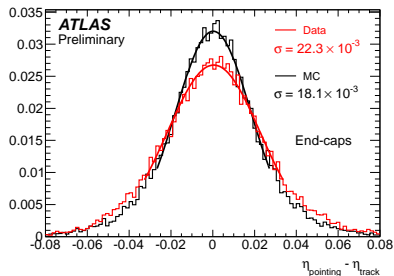
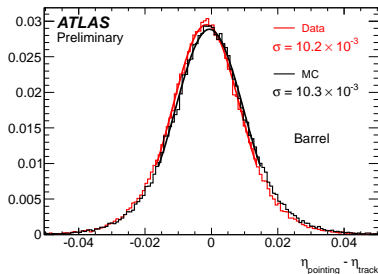
Invariant mass distribution in data, with the background exponential fit for the 5 categories : Unconverted-central, Unconverted-rest, Converted-central, Converted-rest and Converted-transition. The observed mass distribution in each category is well described by the exponential model

$H \rightarrow \gamma\gamma$ - Expected mass distributions



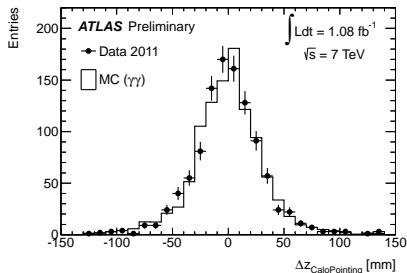
- Expected mass distribution for a 120 GeV Higgs boson signal for the 5 categories
- The parameters of the mass resolution fit are also shown
- The increase of resolution as well as non Gaussian-tails when moving from the best categories to the worse ones is clearly visible

$H \rightarrow \gamma\gamma$ - Systematics from photon pointing



- Comparison between the direction measurement from the calorimeter pointing and the more precise track direction for a control sample of $Z \rightarrow ee$ decays, for electrons in the barrel and electrons in the end-cap. Data are compared to predictions from the simulation.
- In the barrel, the measured resolution agrees well with the predicted one, in the end-cap there is a $\approx 20\%$ worse resolution in the data, coming from a remaining modulation of the layer 2 measurement in the data as a function of η

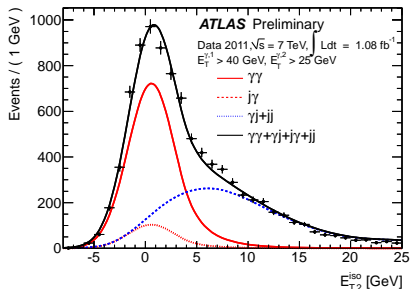
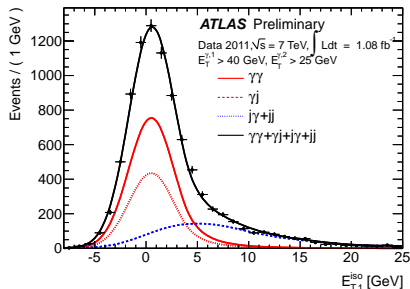
$H \rightarrow \gamma\gamma$ - Systematics from photon pointing



- Comparison between the two estimates of the primary vertex z positions using diphoton events where both photons are unconverted in the barrel, i.e both positions are derived from the calorimeter pointing.
- The resolution observed in data is in good agreement with the prediction from the simulation (diphoton MC).
- The RMS spread of the z is about 3 cm, corresponding to $\approx 1.5\text{cm}$ resolution for the average of the two z .

$H \rightarrow \gamma\gamma$ - Composition of the continuum spectrum

Using template fit method



- Isolation distribution of the data, for the leading and for the subleading photon, fitted with the templates for the various background components.
- The diphoton signal giving two isolated photon candidates is clearly visible and well-separated from the reducible backgrounds.
- This template fit method is an alternative to the double side-band method.

The mass resolution for the signal is modelled by the sum of a Crystal Ball function (for the bulk of the events) and a Gaussian with wide sigma (to model the far outliers in the distribution)

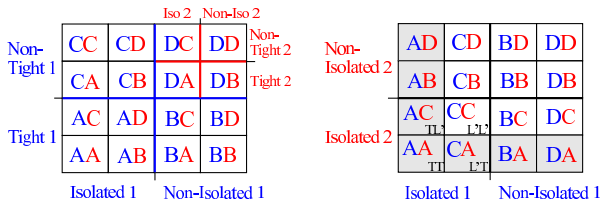
The Crystal Ball function is defined as :

$$N \cdot \begin{cases} e^{-t^2/2} & \text{if } t > -\alpha_{CB} \\ \left(\frac{n_{CB}}{|\alpha_{CB}|}\right)^{n_{CB}} \cdot e^{-|\alpha_{CB}|^2/2} \cdot \left(\frac{n_{CB}}{|\alpha_{CB}|} - |\alpha_{CB}| - t\right)^{-n_{CB}} & \text{otherwise} \end{cases}$$

where $t = (m_{\gamma\gamma} - \mu_{CB})/\sigma_{CB}$, N is a normalization parameter, μ_{CB} is the peak of the Gaussian distribution, σ_{CB} represents the Gaussian mass resolution for the core component, and n_{CB} and α_{CB} parametrize the non-Gaussian tail.

- Principle : estimate purity of isolated and tightly-identified photon pairs by extrapolating the backgrounds from control regions to the signal region
 - Initial sample : events with a pair of *Loose'* photons, composed of $\gamma\gamma$, γj , $j\gamma$ and jj
 - *Loose'* defined by relaxing 4/5 (w_{S3} , F_{side} , ΔE , E_{ratio}) strip variables wrt *Tight*
-
- The 2 selected γ candidates in each event are classified simultaneously
 - Each photon can either pass or fail the *Tight* identification and pass or fail the isolation cut \rightarrow 4 regions for one γ , and $4 \times 4 = 16$ combinations for the 2 γ , always distinguishing between leading and sub-leading candidate
 - The following nomenclature is used
 - *A* labels if a photon is isolated and identified as *Tight*
 - *B* labels the case when a *Tight* photon is non-isolated
 - *C* mean the photon fails the *Tight* requirement but is isolated
 - *D* is the case when the photon fails the isolation cut and the *Tight* identification
 - The 16 regions defined by that are thus :
 - Signal region N_{AA} (TITI),
 - and 15 background control regions N_{AB} , N_{DC} , ...

$H \rightarrow \gamma\gamma - 2 \times 2D$ Sideband Method



The 16 regions in the improved 2x2D method in two different illustrations. The first (second) letter labels the leading (subleading) photon. On the left the regions are sorted first for the leading photon (blue) and then the subleading photon (red). On the right is the same information but in the isolation plane of both photons, and the pattern indicating the quality requirements is indicated in black. The regions used in the calculations are filled with grey.

$H \rightarrow \gamma\gamma - 2 \times 2D$ Sideband Method

In the method applied in this note, however, not the complete information available is exploited.

Neglecting different fake rates for jets in jj events compared to γj (or $j\gamma$) events and potential jj or $\gamma\gamma$ correlations, one can truncate the information to 7 regions : N_{AA} , N_{AB} , N_{AC} , N_{AD} , N_{BA} , N_{CA} and N_{DA} , which can be folded into two 2D sidebands.



The two 2D sidebands corresponding to the leading photon (left) and subleading photon (right) used in the improved method as described by the text.